JACS
JOURNAL OF THE AMERICAN CHEMICAL SOCIETY
Communication
pubs.acs.org/JACS

Selective Synthesis of Molecular Borromean Rings: Engineering of Supramolecular Topology via Coordination-Driven Self-Assembly

Taegeun Kim,[†,∥] Nem Singh,[†,∥] Jihun Oh,[†] Eun-Hee Kim,[§] Jaehoon Jung,*[,†] Hyunuk Kim,*[,‡] and Ki-Whan Chi*[,†]

[†]Department of Chemistry, University of Ulsan, Ulsan 44610, Republic of Korea
[§]Protein Structure Group, Korea Basic Science Institute, Ochang, Chungbuk 28119, Republic of Korea
[‡]Energy Materials and Convergence Research Department, Korea Institute of Energy Research, Daejeon 34129, Republic of Korea

Supporting Information

ABSTRACT: Molecular Borromean rings (BRs) is one of the rare topology among interlocked molecules. Template-free synthesis of BRs via coordination-driven self-assembly of tetracene-based Ru(II) acceptor and ditopic pyridyl donors is reported. NMR and single-crystal XRD analysis observed sequential transformation of a fully characterized monomeric rectangle to molecular BRs and vice versa. Crystal structure of BRs revealed that the particular topology was enforced by the appropriate geometry of the metallacycle and multiple parallel-displaced $\pi-\pi$ interactions between the donor and tetracene moiety of the acceptor. Computational studies based on density functional theory also supported the formation of BRs through dispersive intermolecular interactions in solution.

In the past two decades abiological self-assembly has emerged as a well-established method for the rational design of supramolecules by the independent pioneering work of Stang,[1] Fujita,[2] Raymond,[3] Mirkin,[4] and others[5] using the metal−ligand coordination. The coordination-driven self-assembly approach is now competing and complimenting the covalent synthetic methods for realizing the topologically complicated fascinating molecular architectures.[6] This approach is now being frequently used in the synthesis of commonly known threaded architectures such as catenanes, rotaxanes, and links.[7−9] The synthesis of [2]catenanes has become routine,[6] whereas the synthesis of more topologically complex, mechanically interlocked molecular architectures such as Borromean rings (BRs),[10] Solomon link,[11] star of David catenane,[12] and pentafoil knots[13] is still a great challenge. Molecular BRs consist of three chemically independent rings that are locked in such a way that no two of the three rings are linked with each other as a Hopf link and opening of any one ring unlinks all.[14] Recently the configuration of BRs was selected for the new logo of International Mathematical Union.[15] BRs topology has been previously observed in DNA[16] and crystal packing,[17] and BRs intermediates[18] have also been reported. However, there are only two strategies known in the literature for the synthesis of discrete real (chemically nonconnected) molecular BRs. Stoddart reported the first BRs associated with six Zn(II) metal coordination,[19] subsequent demetalation provided real BRs along with free and open rings.[20] Jin reported another strategy using Cu(II) derived acceptor to produce real and associated BRs. However, the presence of paramagnetic Cu(II) nuclei restricted their NMR analysis to studying their purity and interconversion to monomeric rectangles (Figure 1).[21]

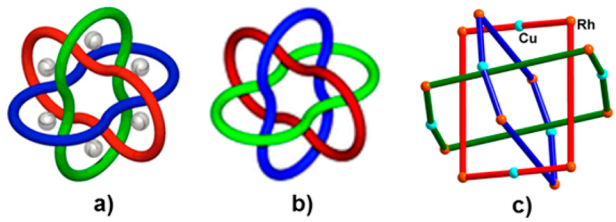

Figure 1. Reported examples of BRs: (a) metal associated BRs, (b) real BRs after demetalation, (c) real BRs wearing paramagnetic Cu(II) ions.

With suitable modifications in the length, shape, and functionality of the donor, we recently reported the template-free synthesis of a molecular Solomon link,[22a] a Hopf's link,[22b] an interlocked prismatic cage,[22c] and a noncatenane "rectangle-in-rectangle"[22d] through the combined strategy of coordination driven self-assembly and $\pi-\pi$ stacking. Here we report the template-free self-assembly of BRs and solvent-induced sequential interconversion of BRs to a monomeric ring by carefully selecting the dimensions and functionality of the donor and acceptor. The BRs topology was obtained from the coordination-driven self-assembly of an arene-Ru(II) acceptor **A** and a ditopic ligand, 1,4-bis(4-pyridinylethynyl) benzene ($\mathbf{L_1}$) (Scheme 1).

The stirring of a 1:1 mixture (0.5 mM) of acceptor **A** and ligand $\mathbf{L_1}$ in CD_3OD for 6 h at room temperature resulted in a clear greenish solution. The neat ^1H NMR spectrum of the solution clearly indicated the quantitative self-assembly of molecular rectangle **1** as α- and β-pyridyl protons were shifted from 8.67 and 7.55 ppm to 8.52 and 7.33 ppm, respectively (Figures 2 and S1−S2). Similarly, the phenylene protons (labeled as H_{L1}) were also shifted to 7.30 ppm from 7.64 ppm in the $\mathbf{L_1}$. The prominent peaks at m/z = 742.76 $[\mathbf{1}\text{-}3OTf]^{3+}$ in the ESI-MS analysis confirmed the formation of **1**, which were in good agreement with the theoretical isotopic distributions of

Received: May 3, 2016
Published: June 23, 2016

DOI: 10.1021/jacs.6b04545
J. Am. Chem. Soc. 2016, 138, 8368−8371

Scheme 1. Self-Assembly and Interconversion of BRs and Monomeric Rectangles

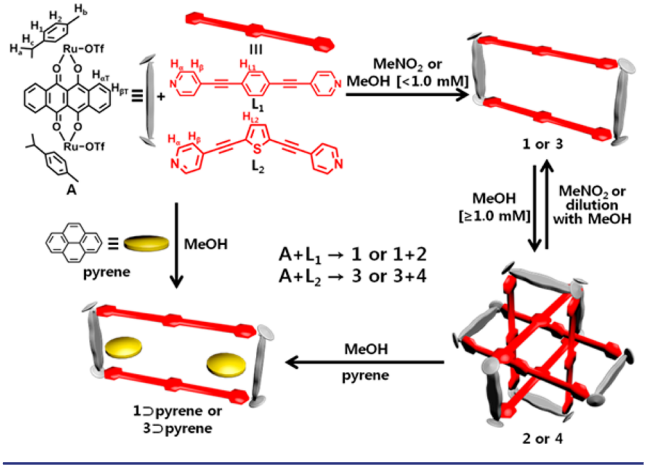

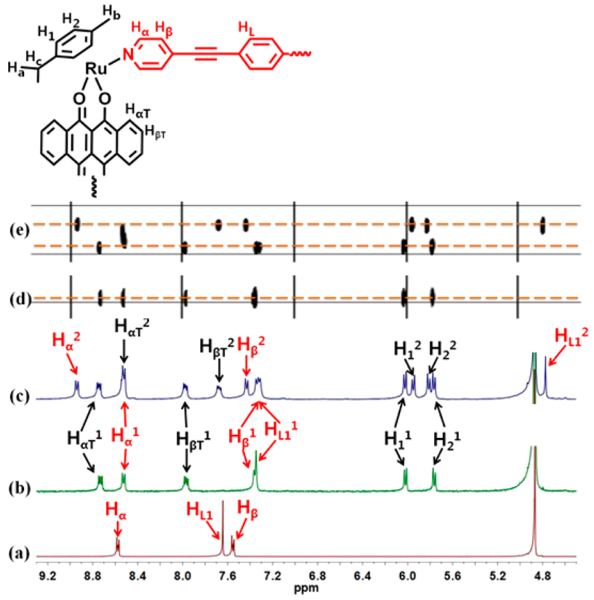

Figure 2. Partial ^{1}H NMR in CD_3OD of (a) donor (b) self-assembled monomeric rectangle **1** [0.5 mM], (c) mixture of **1** and BRs **2** [3.0 mM], (d) ^{1}H DOSY NMR of **1** [0.5 mM], and (e) ^{1}H DOSY NMR of **1** + **2** [3.0 mM].

1 (Figure S3). Upon increasing the reaction concentration to 1.0 mM, new peaks were observed along with peaks from **1** in the ^{1}H NMR spectrum that indicated the formation of a new compound (Figure 5S). The similar reaction in CD_3NO_2 also resulted in only **1** unaffected by concentration (Figure S2). This observation prompted us to carry out reactions in CD_3OD in various concentrations from 0.5 to 8.0 mM (solubility was poor beyond 6.0 mM) (Figure S5). The reaction carried out at 6.0 mM provided the maximum concentration (56%) of the new compound. The ^{1}H NMR spectral pattern of new compound was similar to that of **1** except for the fact that the phenylene protons (labeled as H_{L1}) were highly shifted upfield from 7.64 to 4.77 ppm (Figure 2).

The prominent peaks in the ESI-MS spectrum at m/z = 2525.86 $[\mathbf{2}\text{-}3\text{OTf}]^{3+}$ and the perfect agreement with the theoretical isotopic distributions confirmed the presence of BRs **2** (Figure S6). The structures of BRs **2** and monomeric rectangle **1** were confirmed in solution by DOSY, ROESY, HSQC, and HMBC 2D NMR (Figures S1–S19) combined with ESI-MS analysis. The strong upfield shift of phenylene protons in the ^{1}H NMR spectrum was a result of parallel-displaced $\pi-\pi$ stacking with the tetracene moiety of acceptor **A** and CH$\cdots\pi$ interactions with the pyridyl ring of another rectangle. The DOSY NMR spectrum of **1** [0.5 mM] in CD_3OD was recorded and revealed a diffusion coefficient (D) of 5.3×10^{-10} m^2 s^{-1}. The DOSY NMR spectrum of mixture of **1** + **2** [3.0 mM] in CD_3OD also confirmed the NMR signals associated with two diffusion coefficients at $D = 5.1 \times 10^{-10}$ m^2 s^{-1} for **1** and 3.9×10^{-10} m^2 s^{-1} for **2** (Figures 2 and S10–S13). The ^{1}H–^{1}H ROSEY spectra of **1** [0.5 mM] and **1** + **2** [3.0 mM] in CD_3OD also showed all the possible coupling interactions in the structure of **1** and BRs **2**. The coupling interactions of phenylene protons of donors with α-,β-tetracene protons of acceptor moiety were also observed, which was possible only in the case of BRs topology of **2** (Figures S14–S15).

To identify the driving forces behind the formation of BRs, we tried the self-assembly of ligand $\mathbf{L_1}$ with other similar acceptors,[22a] but none of them resulted in BRs topology. In search of replacing $\mathbf{L_1}$ to get increased yield, we tried various ligands and found 2,5-bis(4-pyridinylethynyl)thiophene ($\mathbf{L_2}$) provided much better yield up to 65% of BRs. Ligand $\mathbf{L_1}$ was replaced with $\mathbf{L_2}$ in identical reactions which earlier produced **1** and **2**, resulting in the formation of new compounds **3** and **4**. The combined NMR study and prominent peaks at m/z = 746.73 $[\mathbf{3}\text{-}3\text{OTf}]^{3+}$ and m/z = 1463.53 $[\mathbf{4}\text{-}5\text{OTf}]^{5+}$ in the ESI-MS analysis confirmed the formation of monorectangle **3** and BRs **4**, which were in good agreement with their theoretical isotopic distributions (Figures S20–S37). In the search of getting pure BRs, we tried the self-assembly in different solvents and mixtures of solvents in which **3** and **4** were soluble. Only D_2O added in CD_3OD solution provided improved yield of BRs. The 6.0 mM reaction mixture in CD_3OD was stirred for 6 h, and then from this solution six different sets of reactions were prepared by adding D_2O and adjusting the CD_3OD:D_2O ratio up to 9:6 (up to allowed solubility). The resulting reaction mixtures were further stirred for 6 h, and ^{1}H NMR was recorded (Figure 3). The NMR spectra showed a gradual increase in the percentage of BRs upon addition of D_2O, which increased up to 87% in the CD_3OD:D_2O ratio of 9:6.

The DOSY NMR spectrum of mixture of **3** + **4** [4.0 mM] in CD_3OD also revealed two diffusion coefficients at D = 5.5 ×

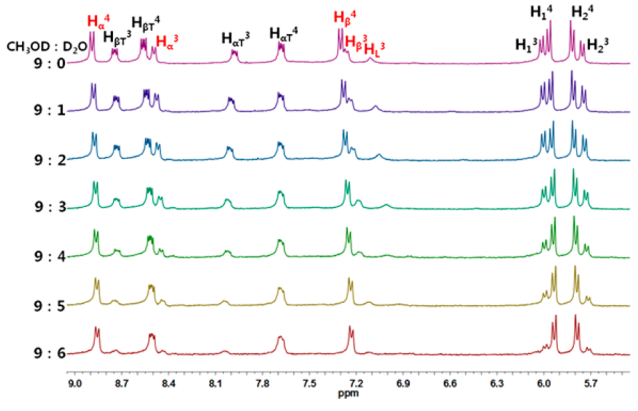

Figure 3. Partial ^{1}H NMR spectra of mixture of **3** + **4** in CD_3OD[6.0 mM] showing transformation to 87% of BRs **4** upon increasing the CD_3OD:D_2O ratio up to 9:6.

DOI: 10.1021/jacs.6b04545
J. Am. Chem. Soc. 2016, 138, 8368–8371

10^{-10} m^2 s^{-1} for **3** and 4.2×10^{-10} m^2 s^{-1} for **4**, whereas DOSY NMR of **4** obtained in CD_3OD:D_2O (9:6) showed the diffusion coefficient at $D = 1.5 \times 10^{-10}$ m^2 s^{-1} for NMR signals associated with BRs **4** (Figures S27–S30). The coupling interactions of β-thiophene protons of donors with α-,β-tetracene protons of acceptor moiety in the ^1H–^1H ROSEY spectra of **3** + **4** [4.0 mM] in CD_3OD were also observed to confirm BRs topology of **4** (Figures S31 and S32). The transformation of monorectangle **3** to BRs **4** upon sequential addition of D_2O was probably instigated by the hydrophobic effect. The metallacycles due to the presence of hydrophobic moieties would come closer to reduce the solvent accessible surface area in order to avoid exposure to D_2O. Computational calculations of solvent effect also suggested a decrease in solvent accessible surface area by ~172 $Å^2$ due to the formation of BRs **2** (SI).

To understand the role of π–π interactions in formation of BRs, 0.5–8.0 equiv of pyrene was added to the previously prepared 4.0 mM solutions of **1** + **2** and **3** + **4** in CD_3OD. The resulting reaction mixtures were further stirred for 2 h at 45 °C, and NMR was recorded. The NMR data clearly show the gradual transformation of BRs to single rectangle upon increasing the concentration of pyrene (Figures S38 and S39). The BRs completely transformed into single rectangles by interacting with 8.0 equiv of pyrene. Solution of **3** + **4** in CD_3OD upon sequential dilution with CD_3OD was also resulted in pure monomeric rectangle **3** (Figures S40).

The single-crystal X-ray diffraction (scXRD) analysis unambiguously confirmed the structures of **1** encapsulated with two molecules of pyrene, **3** (obtained from the CD_3NO_2 solution), and BRs **2** and **4** in the solid state (Figure 4).

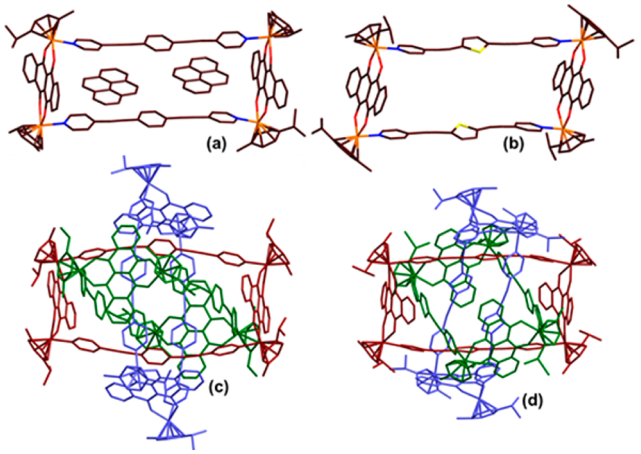

Figure 4. X-ray crystal structures of (a) **1** ⊃ (2·pyrene), (b) **3**, (c) **2**, and (d) **4**. Hydrogen atoms and counteranions are omitted for clarity.

Considering the metallacycles as rectangles, the scXRD analysis confirmed the molecular structure of **2** with pyritohedral symmetry (T_h), wherein the three rings were found to be linked with the topology of BRs. Each of the three equivalent rings adopted a distorted rectangle-like conformation with an average length and width (Ru–Ru distance) of 20.1 and 8.1 Å respectively. The three chemically nonconnected distorted rectangles were held together by CH···π (2.9 Å) interactions and multiple parallel-displaced π–π (3.5 Å) interactions between phenyl-ethynyl-pyridinyl moieties of the donor and tetracene moieties of the acceptor (Figure S44–S45). The structure of **4** was also found similar to BRs **2** with average rectangular dimensions of 19.6 and 7.9 Å. In the structure of **1**, two pyrene molecules were found to be encapsulated and strongly interacted with the ethynyl-pyridinyl moiety stabilized via parallel-displaced π–π stacking (3.5 Å) and via CH···π (2.7 Å) interactions in edge-to-face fashion with the tetracene moiety of the acceptor. Interestingly, the donor moieties of the rectangle were curved outside in the case of BRs **2** and **4**, slightly toward the inside in **1**⊃(2·pyrene), and almost straight in the case of monomeric rectangle **3** (Figures S42–S48). This observation clearly indicated that the driving forces in the formation of BRs are multiple π–π and CH···π interactions, which is also supported by the theoretically obtained spatial distribution of noncovalent interaction (NCI) by plotting the iso-surfaces of reduced density gradient as shown in Figure S49.[23]

In conclusion, template-free synthesis of molecular BRs was achieved via coordination-driven self-assembly and parallel-displaced π–π stacking of aromatic rings. Various acceptors and donors in different solvents and combination of solvents were tried, but tetracene-based acceptor and thiophene-derived donor in methanol–water solution were found to be the best combination to get the desired topology. The self-assembly in nitromethane resulted only in monomeric rectangle regardless of concentration. In methanol, whereas only a single rectangle was obtained in dilute reaction condition, BRs gradually started forming upon increasing the reaction concentration beyond 1.0 mM. The formation of BRs was inhibited by the presence of π-electron-rich pyrene template shown by NMR analysis and X-ray crystal structure of the monomeric rectangle encapsulated with pyrene. The real molecular BRs were characterized by scXRD analysis in solid-state along with elegant demonstration of linking and unlinking by NMR analysis in solution. When all the NMR, scXRD, and computational studies were combined, the driving forces for the formation of BRs were found to be CH···π interactions and multiple parallel-displaced π–π interactions with appropriate geometry of donor and acceptor. We demonstrated the engineering of complex supramolecular topology through controlling concentration, solvent, template, and the functionality of donor and acceptor.

■ ASSOCIATED CONTENT

Supporting Information

The Supporting Information is available free of charge on the ACS Publications website at DOI: 10.1021/jacs.6b04545.

Details of the synthesis, spectroscopic data, and computation details for **1**–**4** (PDF)
Crystallographic data (CIF)

■ AUTHOR INFORMATION

Corresponding Authors

*jjung2015@ulsan.ac.kr
*hyunuk@kier.re.kr
*kwchi@ulsan.ac.kr

Author Contributions

‖These authors contributed equally.

Notes

The authors declare no competing financial interest.

■ ACKNOWLEDGMENTS

This work was supported by the Basic Science Research program through the National Research Foundation of Korea (2016R1A2B4007433 to K.W.C, 2014R1A1A2007897 to N.S.,

DOI: 10.1021/jacs.6b04545
J. Am. Chem. Soc. 2016, 138, 8368–8371

and 2015R1C1A1A01052947 to J.J.). Priority Research Centers program (2009-0093818) through the NRF is also financially appreciated. H.K. thanks to Research and Development Program of KIER (B6-2484). XRD experiments using the synchrotron radiation were performed at the Pohang Accelerator Laboratory.

REFERENCES

(1) (a) Leininger, S.; Olenyuk, B.; Stang, P. J. *Chem. Rev.* **2000**, *100*, 853. (b) Seidel, S. R.; Stang, P. J. *Acc. Chem. Res.* **2002**, *35*, 972. (c) Northrop, B. H.; Zheng, Y.-R.; Chi, K.-W.; Stang, P. J. *Acc. Chem. Res.* **2009**, *42*, 1554. (d) Chakrabarty, R.; Mukherjee, P. S.; Stang, P. J. *Chem. Rev.* **2011**, *111*, 6810. (e) Cook, T. R.; Vajpayee, V.; Lee, M. H.; Stang, P. J.; Chi, K.-W. *Acc. Chem. Res.* **2013**, *46*, 2464. (f) Cook, T. R.; Stang, P. J. *Chem. Rev.* **2015**, *115*, 7001.

(2) (a) Fujita, M. *Chem. Soc. Rev.* **1998**, *27*, 417. (b) Fujita, M.; Tominaga, M.; Hori, A.; Therrien, B. *Acc. Chem. Res.* **2005**, *38*, 369. (c) Yoshizawa, M.; Klosterman, J. K.; Fujita, M. *Angew. Chem., Int. Ed.* **2009**, *48*, 3418.

(3) (a) Pluth, M. D.; Raymond, K. N. *Chem. Soc. Rev.* **2007**, *36*, 161. (b) Caulder, D. L.; Raymond, K. N. *Acc. Chem. Res.* **1999**, *32*, 975.

(4) (a) Gianneschi, N. C.; Masar, M. S., III; Mirkin, C. A. *Acc. Chem. Res.* **2005**, *38*, 825. (b) Holliday, B. J.; Mirkin, C. A. *Angew. Chem., Int. Ed.* **2001**, *40*, 2022.

(5) (a) McConnell, A. J.; Wood, C. S.; Neelakandan, P. P.; Nitschke, J. R. *Chem. Rev.* **2015**, *115*, 7729. (b) Zarra, S.; Wood, D. M.; Roberts, D. A.; Nitschke, J. R. *Chem. Soc. Rev.* **2015**, *44*, 419. (c) Han, Y. F.; Jin, G. X. *Chem. Soc. Rev.* **2014**, *43*, 2799. (d) Han, Y.-F.; Jin, G.-X. *Acc. Chem. Res.* **2014**, *47*, 3571. (e) Mukherjee, S.; Mukherjee, P. S. *Chem. Commun.* **2014**, *50*, 2239. (f) Singh, N.; Jo, J.-H.; Song, Y. H.; Kim, H.; Kim, D.; Lah, M. S.; Chi, K.-W. *Chem. Commun.* **2015**, *51*, 4492. (g) Dolomanov, O. V.; Blake, A. J.; Champness, N. R.; Schröder, M.; Wilson, C. *Chem. Commun.* **2003**, 682.

(6) (a) Forgan, R. S.; Sauvage, J.-P.; Stoddart, J. F. *Chem. Rev.* **2011**, *111*, 5434. (b) Gil-Ramirez, G.; Leigh, D. A.; Stephens, A. J. *Angew. Chem., Int. Ed.* **2015**, *54*, 6110. (c) De, S.; Mahata, K.; Schmittel, M. *Chem. Soc. Rev.* **2010**, *39*, 1555.

(7) (a) *Molecular Catenanes, Rotaxanes, and Knots: A Journey Through the World of Molecular Topology*; Sauvage, J.-P., Dietrich-Buchecker, C., Eds.; Wiley-VCH: Weinheim, Germany, 1999. (b) Fujita, M. *Acc. Chem. Res.* **1999**, *32*, 53.

(8) (a) Wood, C. S.; Ronson, T. K.; Belenguer, A. M.; Holstein, J. J.; Nitschke, J. R. *Nat. Chem.* **2015**, *7*, 354. (b) Kottas, G. S.; Clarke, L. I.; Horinek, D.; Michl, J. *Chem. Rev.* **2005**, *105*, 1281.

(9) Beves, J. E.; Blight, B. A.; Campbell, C. J.; Leigh, D. A.; McBurney, R. T. *Angew. Chem., Int. Ed.* **2011**, *50*, 9260.

(10) (a) Cantrill, S. J.; Chichak, K. S.; Peters, A. J.; Stoddart, J. F. *Acc. Chem. Res.* **2005**, *38*, 1. (b) Meyer, C. D.; Forgan, R. S.; Chichak, K. S.; Peters, A. J.; Tangchaivang, N.; Cave, G. W. V.; Khan, S. I.; Cantrill, S. J.; Stoddart, J. F. *Chem. - Eur. J.* **2010**, *16*, 12570.

(11) (a) Ibukuro, F.; Fujita, M.; Yamaguchi, K.; Sauvage, J.-P. *J. Am. Chem. Soc.* **1999**, *121*, 11014. (b) Beves, J. E.; Danon, J. J.; Leigh, D. A.; Lemonnier, J.-F.; Vitorica-Yrezabal, I. J. *Angew. Chem., Int. Ed.* **2015**, *54*, 7555. (c) Ponnuswamy, N.; Cougnon, F. B. L.; Pantoş, D. G.; Sanders, J. K. M. *J. Am. Chem. Soc.* **2014**, *136*, 8243. (d) Prakasam, T.; Lusi, M.; Elhabiri, M.; Platas-Iglesias, C.; Olsen, J. C.; Asfari, Z.; Cianférani-Sanglier, S.; Debaene, F.; Charbonnière, L. J.; Trabolsi, A. *Angew. Chem., Int. Ed.* **2013**, *52*, 9956.

(12) Leigh, D. A.; Pritchard, R. G.; Stephens, A. J. *Nat. Chem.* **2014**, *6*, 978.

(13) (a) Ayme, J.-F.; Beves, J. E.; Leigh, D. A.; McBurney, R. T.; Rissanen, K.; Schultz, D. *Nat. Chem.* **2012**, *4*, 15. (b) Ayme, J.-F.; Beves, J. E.; Leigh, D. A.; McBurney, R. T.; Rissanen, K.; Schultz, D. *J. Am. Chem. Soc.* **2012**, *134*, 9488.

(14) Adams, C. C.*The knot book: an elementary introduction to the mathematical theory of knots*American Mathematical Soc.: Providence, RI, 2004

(15) Gunn, C.; Sullivan, J. M. The Borromean Rings: A video about the new IMU logo. Proceedings of the *Bridges (Leeuwarden)*, July 24–28, 2008, Leeuwarden, The Netherlands; p 63.

(16) Mao, C.; Sun, W.; Seeman, N. C. *Nature* **1997**, *386*, 137.

(17) Thorp-Greenwood, F. L.; Kulak, A. N.; Hardie, M. J. *Nat. Chem.* **2015**, *7*, 526. (b) Liantonio, R.; Metrangolo, P.; Meyer, F.; Pilati, T.; Navarrini, W.; Resnatti, G. *Chem. Commun.* **2006**, 1819.

(18) (a) Loren, J. C.; Yoshizawa, M.; Haldimann, R. F.; Linden, A.; Siegel, J. S. *Angew. Chem., Int. Ed.* **2003**, *42*, 5702. (b) Schalley, C. A. *Angew. Chem., Int. Ed.* **2004**, *43*, 4399.

(19) (a) Chichak, K. S.; Cantrill, S. J.; Pease, A. R.; Chiu, S. H.; Cave, G. W. V.; Atwood, J. L.; Stoddart, J. F. *Science* **2004**, *304*, 1308. (b) Chichak, K. S.; Peters, A. J.; Cantrill, S. J.; Stoddart, J. F. *J. Org. Chem.* **2005**, *70*, 7956.

(20) Peters, A. J.; Chichak, K. S.; Cantrill, S. J.; Stoddart, J. F. *Chem. Commun.* **2005**, 3394.

(21) (a) Huang, S.-L.; Lin, Y.-J.; Andy Hor, T. S.; Jin, G.-X. *J. Am. Chem. Soc.* **2013**, *135*, 8125. (b) Huang, S.-L.; Lin, Y.-L.; Li, Z.-H.; Jin, G.-X. *Angew. Chem., Int. Ed.* **2014**, *53*, 11218.

(22) (a) Song, Y. H.; Singh, N.; Jung, J.; Kim, H.; Kim, E.-H.; Cheong, H.-K.; Kim, Y.; Chi, K.-W. *Angew. Chem., Int. Ed.* **2016**, *55*, 2007. (b) Lee, H.; Elumalai, P.; Singh, N.; Kim, H.; Lee, S. U.; Chi, K.-W. *J. Am. Chem. Soc.* **2015**, *137*, 4674. (c) Mishra, A.; Dubey, A.; Min, J. W.; Kim, H.; Stang, P. J.; Chi, K.-W. *Chem. Commun.* **2014**, *50*, 7542. (d) Vajpayee, V.; Song, Y. H.; Cook, T. R.; Kim, H.; Lee, Y.; Stang, P. J.; Chi, K.-W. *J. Am. Chem. Soc.* **2011**, *133*, 19646.

(23) DFT computations were performed to study the intermolecular interactions in BRs **2**. The binding energies (BE) evaluated using three different hybrid functionals were −127.8 (ωB97X-D), −58.9 (M06-2X), and 26.6 kcal/mol (PBE0), with the geometry determined by scXRD. The variation of BE of employed methods, according to the performance in describing NCI, clearly indicates that the NCI plays a crucial role in the formation of BRs (see SI for computation details).

DOI: 10.1021/jacs.6b04545
J. Am. Chem. Soc. 2016, 138, 8368–8371